A LETTERS JOURNAL EXPLORING THE FRONTIERS OF PHYSICS

OFFPRINT

Topology of force networks in compressed granular media

L. Kondic, A. Goullet, C. S. O'Hern, M. Kramar, K. Mischaikow and R. P. Behringer

EPL, **97** (2012) 54001

epl

A Letters Journal Exploring the Frontiers of Physics

AN INVITATION TO SUBMIT YOUR WORK

www.epljournal.org

The Editorial Board invites you to submit your letters to EPL

EPL is a leading international journal publishing original, high-quality Letters in all areas of physics, ranging from condensed matter topics and interdisciplinary research to astrophysics, geophysics, plasma and fusion sciences, including those with application potential.

The high profile of the journal combined with the excellent scientific quality of the articles continue to ensure EPL is an essential resource for its worldwide audience. EPL offers authors global visibility and a great opportunity to share their work with others across the whole of the physics community.

Run by active scientists, for scientists

EPL is reviewed by scientists for scientists, to serve and support the international scientific community. The Editorial Board is a team of active research scientists with an expert understanding of the needs of both authors and researchers.

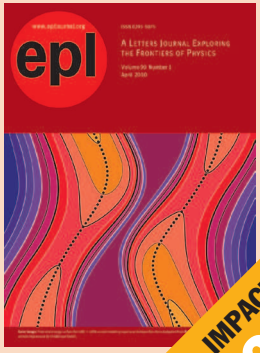

IMPACT FACTOR 2.753*

*As ranked by ISI 2010

IMPACT FACTOR
2.753*
* As listed in the ISI® 2010 Science Citation Index Journal Citation Reports

OVER
500 000
full text downloads in 2010

30 DAYS
average receipt to online publication in 2010

16 961
citations in 2010
37% increase from 2007

"We've had a very positive experience with EPL, and not only on this occasion. The fact that one can identify an appropriate editor, and the editor is an active scientist in the field, makes a huge difference."

Dr. Ivar Martinv
Los Alamos National Laboratory, USA

Six good reasons to publish with EPL

We want to work with you to help gain recognition for your high-quality work through worldwide visibility and high citations.

1. **Quality** – The 40+ Co-Editors, who are experts in their fields, oversee the entire peer-review process, from selection of the referees to making all final acceptance decisions
2. **Impact Factor** – The 2010 Impact Factor is 2.753; your work will be in the right place to be cited by your peers
3. **Speed of processing** – We aim to provide you with a quick and efficient service; the median time from acceptance to online publication is 30 days
4. **High visibility** – All articles are free to read for 30 days from online publication date
5. **International reach** – Over 2,000 institutions have access to EPL, enabling your work to be read by your peers in 100 countries
6. **Open Access** – Articles are offered open access for a one-off author payment

Details on preparing, submitting and tracking the progress of your manuscript from submission to acceptance are available on the EPL submission website **www.epletters.net**.

If you would like further information about our author service or EPL in general, please visit **www.epljournal.org** or e-mail us at **info@epljournal.org**.

EPL is published in partnership with:

European Physical Society | Società Italiana di Fisica | EDP Sciences | IOP Publishing

A Letters Journal Exploring the Frontiers of Physics

March 2012

EPL, **97** (2012) 54001
doi: 10.1209/0295-5075/97/54001

www.epljournal.org

Topology of force networks in compressed granular media

L. Kondic[1(a)], A. Goullet[1], C. S. O'Hern[2], M. Kramar[3], K. Mischaikow[3] and R. P. Behringer[4]

[1] *Department of Mathematical Sciences and Center for Applied Mathematics and Statistics, New Jersey Institute of Technology - Newark, NJ 07102, USA*
[2] *Departments of Mechanical Engineering & Materials Science and Physics, Yale University New Haven, CT 06520-8284, USA*
[3] *Department of Mathematics, Rutgers University - Piscataway, NJ 08854-8019, USA*
[4] *Department of Physics and Center for Nonlinear and Complex Systems, Duke University Durham, NC 27708-0305, USA*

received 5 October 2011; accepted in final form 25 January 2012
published online 28 February 2012

PACS 45.70.-n – Granular systems
PACS 83.10.Rs – Computer simulation of molecular and particle dynamics

Abstract – Using numerical simulations, we investigate the evolution of the structure of force networks in slowly compressed model granular materials in two spatial dimensions. We quantify the global properties of the force networks using the zeroth Betti number B0, which is a topological invariant. We find that B0 can distinguish among force networks in systems with frictionless *vs.* frictional disks and varying size distributions. In particular, we show that 1) the force networks in systems composed of frictionless, monodisperse disks differ significantly from those in systems with frictional, polydisperse disks and we isolate the effect (friction, polydispersity) leading to the differences; 2) the structural properties of force networks change as the system passes through the jamming transition; and 3) the force network continues to evolve as the system is compressed above jamming, *e.g.*, the size of connected clusters with forces larger than a given threshold decreases significantly with increasing packing fraction.

Introduction. – The structure and dynamics of the network of intergrain forces play a dominant role in determining the complex spatiotemporal behavior of dense granular systems, including jamming [1,2], shear banding, impact, and cratering [3]. Force chain networks, which can be visualized in experiments in 2D using photoelastic particles [2] and in 3D using fluorescence techniques coupled with laser-sheet scanning, are often described as filamentary networks of larger than average forces. Discrete element simulations have also been employed to investigate the shape of force distributions, subpopulations of supporting weak and strong force networks, the elastic-like response to point force perturbations, and force-chain correlation lengths [4–7]. A number of studies have also suggested that force chain networks are common to most jammed and glassy materials. For example, force-chain–like structures have been found in other athermal systems such as emulsions and foams, as well as in thermal systems, including colloidal and molecular glasses.

Recent computational studies [8] have also emphasized the strong analogy between random percolation [9] and force chain percolation in granular materials. The results show that the moments of the force cluster size distribution display universal scaling behavior for a wide range of systems, including frictionless and frictional packings, and those that are highly overcompressed and at jamming onset. Related work [10] has also shown that the fractal dimension of the force clusters changes significantly when moving from below to above the jamming transition.

In the current manuscript, we identify features of the force chain networks that can be used to distinguish them, based on the physics of the inter-particle interactions. Using extensive computational studies of model 2D frictionless and frictional granular packings subjected to continuous isotropic compression, we find that particle size polydispersity and frictional properties strongly influence the structure of the force chain networks. In contrast to many prior studies, we consider a wide range of packing fraction, ρ, from dilute systems to those compressed beyond the jamming transition. We illustrate the differences between force chain networks in different systems using a novel measure, Betti numbers, which are global topological invariants that quantify network "connectedness".

(a) E-mail: kondic@njit.edu

Methods. – In the simulations, which are two-dimensional, circular grains are confined to a square domain with rough walls composed of monodisperse particles. The walls move inward at constant speed v_c, which yields packing fractions in the range from 0.6 to 0.9. No annealing of the system is carried out, and gravity is neglected. The disk sizes are chosen from a flat distribution with width $r_p = (r_{max} - r_{min})/r_{ave}$, where r_{ave} is the mean particle radius. The particle-particle (and particle-wall) interactions include normal and tangential components. The normal force between particles i and j is $\mathbf{F}^n_{i,j} = [k_n x - \gamma_n \bar{m} \mathbf{v}_{i,j}]\,\mathbf{n}$, where $r_{i,j} = |\mathbf{r}_{i,j}|$, $\mathbf{r}_{i,j} = \mathbf{r}_i - \mathbf{r}_j$, $\mathbf{n} = \mathbf{r}_{i,j}/r_{i,j}$, and $\mathbf{v}^n_{i,j}$ is the relative normal velocity. The amount of compression is $x = d_{ave} - r_{i,j}$, where $d_{ave} = (d_i + d_j)/2$, d_i and d_j are the diameters of the particles i and j. All quantities are expressed using the average particle diameter, d_{ave}, as the length scale, the binary particle collision time $\tau_c = \pi\sqrt{d_{ave}/(2\,g k_n)}$ as the time scale, and the average particle mass, m, as the mass scale. $\bar{m}$ is the reduced mass, k_n (in units of mg/d_{ave}) is the spring constant set to a value that corresponds to that for photoelastic disks [11], and γ_n is the damping coefficient [12]. The parameters entering the linear force model can be connected to physical properties (Young modulus, Poisson ratio) as described, *e.g.*, in [12].

We implement the commonly used Cundall-Strack model for static friction [13], where a tangential spring is introduced between particles for each new contact that forms at time $t = t_0$. Due to the relative motion of the particles, the spring length, $\boldsymbol{\xi}$ evolves as $\boldsymbol{\xi} = \int_{t_0}^{t} \mathbf{v}^t_{i,j}\,(t')\,\mathrm{d}t'$, where $\mathbf{v}^t_{i,j} = \mathbf{v}_{i,j} - \mathbf{v}^n_{i,j}$. For long-lasting contacts, $\boldsymbol{\xi}$ may not remain parallel to the current tangential direction defined by $\mathbf{t} = \mathbf{v}^t_{i,j}/|\mathbf{v}^t_{i,j}|$ (see, *e.g.*, [14,15]); we therefore define the corrected $\boldsymbol{\xi}' = \boldsymbol{\xi} - \mathbf{n}(\mathbf{n}\cdot\boldsymbol{\xi})$ and introduce the test force $\mathbf{F}^{t*} = -k_t\boldsymbol{\xi}' - \gamma_t \mathbf{v}^t_{i,j}$, where γ_t is the coefficient of viscous damping in the tangential direction (with $\gamma_t = \gamma_n/2$). To ensure that the magnitude of the tangential force remains below the Coulomb threshold, we constrain the tangential force to be $\mathbf{F}^t = \min(\mu_s|\mathbf{F}^n|, |\mathbf{F}^{t*}|)\mathbf{F}^{t*}/|\mathbf{F}^{t*}|$, and redefine $\boldsymbol{\xi}$ if appropriate. To isolate the effects of static friction on the structure of the force chain networks, we also consider a kinetic friction model that includes only viscous damping (*i.e.*, $k_t = 0$).

For the initial configuration, particles are placed on a square lattice and given random initial velocities; we have verified that the results are independent of the distribution and magnitude of these initial velocities. The wall particles move at a uniform (small) inward velocity $v_c = 2.5 \cdot 10^{-5}$. We integrate Newton's equations of motion for both the translation and rotational degrees of freedom using a 4th-order predictor-corrector method with time step $\Delta t = 0.02$. We consider system sizes from $N = 2000$ to 40000 particles with $k_n = 4 \cdot 10^3$, $e_n = 0.5$, $\mu_s = 0.5$, and $k_t = 0$ or $k_t = 0.8k_n$ [16]. The results are ensemble-averaged over 20 realizations characterized by different initial conditions. In addition to the averages, we calculated standard deviations of the computed quantities, and found them to be typically at least an order of magnitude smaller than the means, suggesting that 20 realizations are enough to obtain statistically significant results.

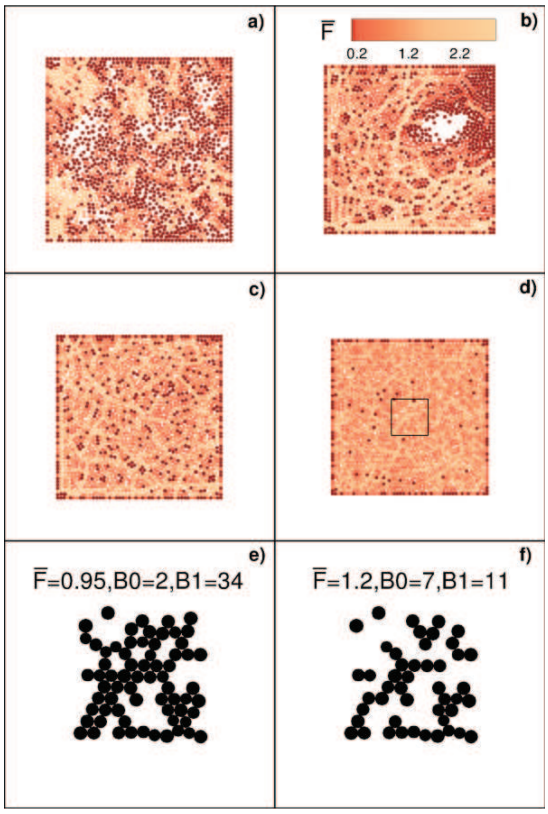

Fig. 1: (Color online) a)–d) The magnitude of the normal force on a given particle scaled by the average normal force $\langle F\rangle$ at four ρ's: 0.62 a), 0.75 b), 0.85 c), and 0.90 d) for $k_t = 0$ and $r_p = 0.2$. e)–f) Central part of panel d) (shown by the black square), where only the particles experiencing normalized force larger than specified force thresholds $\bar{F} = F/\langle F\rangle$ are shown. The values of B0 and B1 are given for illustration. (Attached animation in Quicktime format, `fig1-animation.mov`.)

Results. – Figure 1a)–d) shows several snapshots of the magnitude of the normal force on each particle (normalized by the ρ-dependent average normal force $\langle F\rangle$ in the system) as a function of ρ during compression for $k_t = 0$ and $r_p = 0.2$. Note that each disk is shaded uniformly to a particular hue, corresponding to the (normalized) force threshold $\bar{F} = F/\langle F\rangle$ that it experiences. In this work, we concentrate on normal forces only; tangential forces will be discussed elsewhere. Anticipating future comparison with physical experiments, we time-average the forces over a short time period (10^{-2} s) to mimic the effect of an exposure time, as in photoelastic experiments on compressed granular packings [2]. We proceed by discussing how the tools of algebraic topology can be used to compute objective measures of force chain networks, such as the ones illustrated in fig. 1.

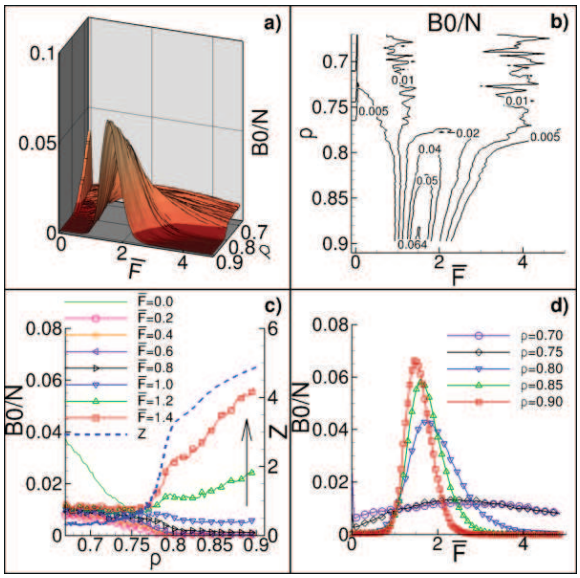

Fig. 2: (Color online) Zeroth Betti number normalized by the number of particles, B0/N, shown as a) contour plot, and b) isoline plot calculated as a function of force threshold $\bar{F}$ and packing fraction ρ. c) Average contact number, Z, and B0/N as a function of ρ calculated at selected $\bar{F}$'s. d) B0/N as a function of $\bar{F}$ calculated at selected ρ. Data from all panels were generated using the model with $k_t = 0$ and $r_p = 0.2$.

The topological quantities that we consider here are Betti numbers, see, *e.g.*, [17]. The zeroth Betti number, B0, measures the number of connected components/clusters formed from mutually contacting particles with normal force magnitudes above given $\bar{F}$. The first Betti number, B1, measures the number of holes, and all higher Betti numbers are zero in 2D. These quantities clearly depend on $\bar{F}$. For example, for $\bar{F} = 0$, B0 measures the network of interparticle contacts. As $\bar{F}$ increases, fewer particles belong to the connected network, and the topology of the resulting structures change. For illustration, figs. 1e) and f) show central part of a domain from fig. 1d), for two values of $\bar{F}$. Calculations of the Betti numbers were performed using CHomP [18]. The software first generates a binary image by thresholding color images of the normal force magnitudes to a particular force threshold as illustrated in fig. 1e)–f). It then measures the connectivity of the resulting images as a function of $\bar{F}$.

Figure 2a), b) shows B0/N, averaged over 20 realizations as a function of $\bar{F}$ and ρ. This figure shows the rich topological structure of the force networks, and nontrivial dependence of B0 on both ρ and $\bar{F}$. In fig. 2c), we show several slices through the 3D plot in fig. 2a) at fixed $\bar{F}$. For $\bar{F} = 0$, we find that the number of connected components strongly decreases as ρ increases, since the number of contacts and cluster size increase. At small ρ, we observe a strong decrease in the number of components at $\bar{F} \neq 0$, suggesting that most of the particles experience very small force. This may not be obvious, given that $\langle F \rangle$ is ρ-dependent, so that for small ρ, $\langle F \rangle$ is small as well. As ρ increases, the number of components grows strongly over a range of force thresholds centered near $\bar{F} \approx 1.4$.

In fig. 2c), we also show the average contact number per particle, Z, as a function of ρ. We find that, for $\bar{F} \gtrapprox 1$, B0$(\rho, \bar{F})$ begins to increase strongly at approximately the same ρ at which Z begins to rise, indicating that the structure of the force network changes significantly close to jamming. Therefore, a strong increase in the number of components/clusters at the force thresholds close to or larger than $\langle F \rangle$, measured by B0, can be used to identify the jamming transition. We discuss the connection between Z and B0 in some more detail below in the context of comparison of the systems differentiated by their polydispersity and friction. For the present case, as the system is further compressed, not only do the particles build up a large number of contacts (illustrated by a decrease of B0 to nearly zero for $\bar{F} \approx 0$), but also, the force network continues to evolve by forming large number of connected clusters at $\bar{F} \sim 1.4$.

In fig. 2d), we plot B0/N as a function of $\bar{F}$ for several values of ρ. This plot shows two key features: i) for $\rho < 0.75$, there is a broad plateau in B0, and ii) as ρ increases, a strong peak in B0 forms, decreases in width, and shifts toward lower $\bar{F}$'s. Our results for B0 indicate a significant change in the force network as ρ increases through the range 0.75–0.80. Similar conclusion can be also reached by considering B1 [19].

Figure 3a) shows the probability density function, $P(\bar{F}, \rho)$. As ρ increases, $P(\bar{F}, \rho)$ evolves from a monotonically decaying function for small ρ to a more complex form for larger ρ, including the formation of a plateau at small force values. We also calculate the average cluster size of particles in contact experiencing normal force magnitudes above a given $\bar{F}$, Np$(\bar{F})$/B0$(\bar{F})$, where $\mathrm{Np}(\bar{F}) = \mathrm{N} \int_{\bar{F}}^{\infty} P(f)\mathrm{d}f$ specifies the total number of particles experiencing a force larger than $\bar{F}$. Figure 3b) shows a dramatic increase in the average cluster size for small $\bar{F}$ and large ρ. (Note that in the present approach, percolating clusters are included in the analysis.) These results show that the average cluster size (measured by Np/B0) becomes comparable to the system size only at small $\bar{F}$. Figure 3b) shows the percolation threshold, defined as the $\bar{F}(\rho)$ at which more than half of the realizations possess a system-spanning cluster in the x- or y-direction. The percolation threshold "envelopes" the region where large clusters are found, as expected. Considering the cluster sizes, however, provides significantly more information compared to what is captured by the percolation threshold alone.

Figures 3c) and d) show in much more detail how Np and the ratio B0/Np vary with ρ and $\bar{F}$. We find that for normal force magnitudes comparable to or larger than the average ($\bar{F} \approx 1$), the clusters are small and contain few particles. The clusters decrease in size as ρ is increased beyond roughly 0.8. This result suggests that the force networks are strongly modified not only at the jamming transition, but also as ρ (or pressure) is further increased.

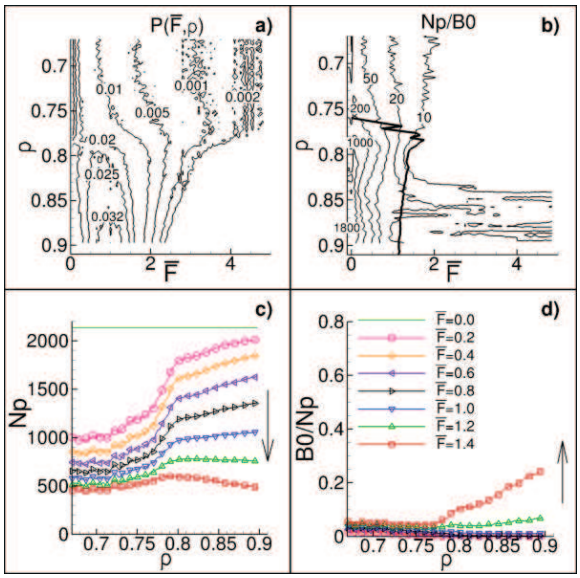

Fig. 3: (Color online) a) Probability density function, $P(\bar{F}, \rho)$ of scaled normal force as a function of ρ; b) average cluster size (number of particles are shown at selected isolines) and the percolation threshold (thick line). System-spanning clusters exist in the region enclosed by the percolation threshold line; c) Number of particles, Np, experiencing a force larger than the specified threshold as a function of ρ; d) B0 normalized by Np as a function of ρ over a range of $\bar{F}$'s. In c) and d), the arrows indicate the direction of increasing $\bar{F}$; the symbols and the line colors are consistent between c) and d). The y-axis label in d) is chosen to facilitate the comparison with other systems, shown in fig. 5. All data presented in this figure are for the model with $k_t = 0$ and $r_p = 0.2$.

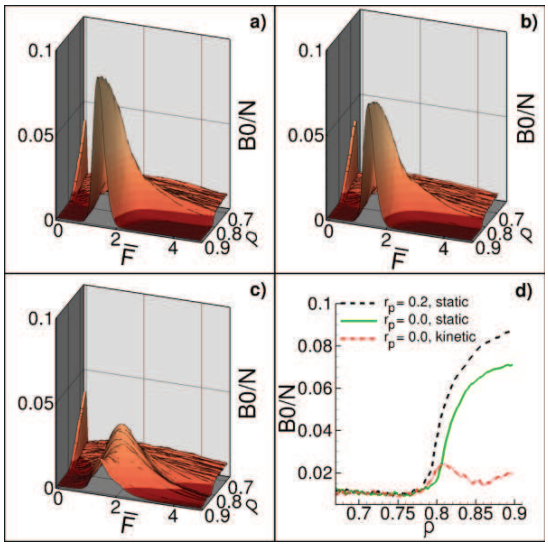

Fig. 4: (Color online) Calculation of B0 for three model granular systems: a) $r_p = 0.2$ with static friction $k_t = 0.8$; b) $r_p = 0.0$ with static friction $k_t = 0.8$; and c) $r_p = 0.0$ with only kinetic friction ($k_t = 0.0$). d) Cross-sections of the 3D B0/N plots at the points where each B0 reaches the maximum value.

We also carried out simulations using larger systems, while always scaling B0 by the number of particles, N. We find excellent scaling of B0 with N, indicating that B0 is extensive. Our results for B0/N are independent of system size.

Considering other system parameters, we find that the influence of the coefficient of restitution has only a minor effect; the stiffness of the particles also turns out not to be important since the time scale it defines is so much faster than other relevant time scales, particularly d_{ave}/v_c. This leaves us with the frictional properties and polydispersity. Figure 4 shows B0/N for three additional model granular systems that probe the effects of these parameters on the structure of force networks. The results for B0/N presented in fig. 4a) for a polydisperse system ($r_p = 0.2$) with static friction ($k_t = 0.8$) suggest that the influence of the friction model on the main topological features for this r_p is minor. In particular, B0 shows qualitatively similar behavior for both $k_t = 0$ and $k_t = 0.8$, although we see a stronger increase in B0 when static friction is present. Therefore, at least for polydisperse systems exposed to isotropic compression, static friction does not influence the features of the force network captured by B0. Figure 4b) shows B0 for a monodisperse system with static friction. For this case also, B0 follows the same qualitative trend as the previous two models. However, the results for B0 in a monodisperse system with kinetic friction only ($k_t = 0$) are qualitatively different. In fig. 4c), we find that B0 initially increases with ρ, but much less rapidly than the other models, and then decreases as ρ is further increased. We will discuss below that this different behavior is related to the formation of crystalline order, which is captured by B0. To illustrate the similarities and differences between the three considered models, we show 2D cross-sections of B0/N at the thresholds where B0 reaches a maximum in fig. 4d). The ρ-dependence of B0 clearly distinguishes the force network structures in different systems.

Figure 5 shows how Np, the number of particles experiencing force larger than a threshold value, and B0/Np, the inverse of the average cluster size, vary as polydispersity and frictional properties are varied. (Note that the results for the polydisperse system with kinetic friction only are shown in fig. 3c) and d).) Considering first Np, we see that the behavior for all systems is similar until ρ reaches values close to 0.8. For larger ρ, we see quantitatively different behavior for the monodisperse system with kinetic friction only (panel e)), although no dramatic difference between the systems is observed. Concentrating now on B0/Np, we see that it strongly increases in the panels b) and d) (static friction either polydisperse or monodisperse), showing that the cluster sizes for $\bar{F}$'s comparable to or larger than $\langle F \rangle$ decrease significantly as ρ is increased. This increase is much stronger compared to the polydisperse system where kinetic friction only is present, shown in fig. 3d). However, for the monodisperse system with kinetic friction only, B0/Np goes through a minimum at $\rho \approx 0.85$, followed by an increase. So, not only is the total number of clusters much smaller for the

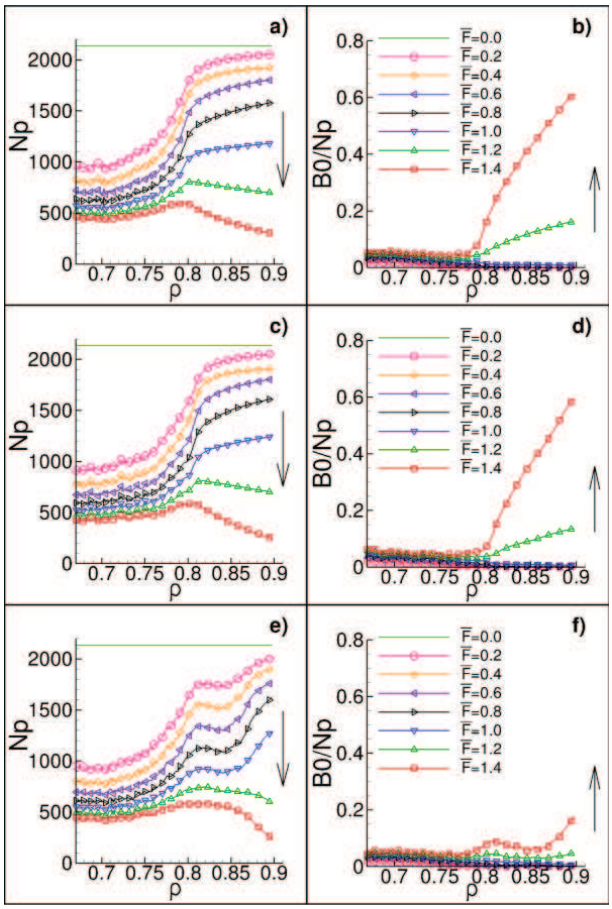

Fig. 5: (Color online) Number of particles, Np, experiencing a force larger than a specified threshold, and B0 normalized by Np for three systems: a) and b) $r_p = 0.2$ with static friction $k_t = 0.8$; c) and d) $r_p = 0.0$ with static friction $k_t = 0.8$; and e) and f) $r_p = 0.0$ with only kinetic friction ($k_t = 0.0$). The arrows indicate the direction of increasing $\bar{F}$.

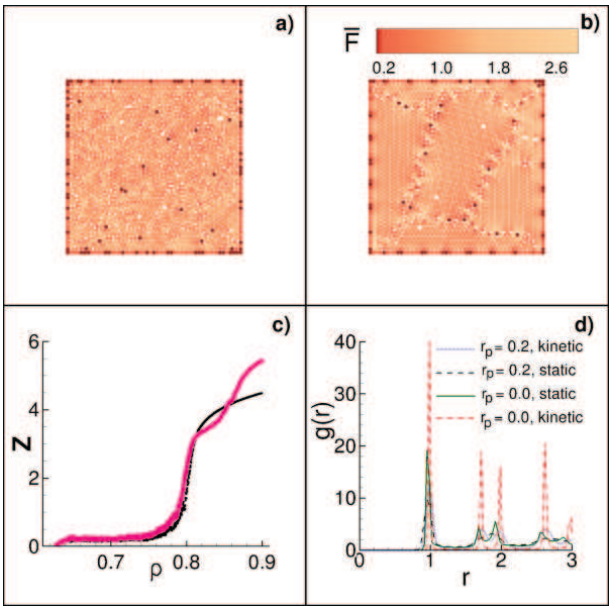

Fig. 6: (Color online) Snapshots at $\rho = 0.9$ of the force network in one realization of a static friction a), and a kinetic friction model for monodisperse particles b). Panel c) shows contact numbers for static (thin black line) and kinetic (thick red line) friction models averaged over 20 realizations of monodisperse systems. Panel d) The radial distribution function for the four model granular systems studied here. (Attached animations in Quicktime format, `fig6a-animation.mov` and `fig6b-animation.mov`.)

monodisperse system with kinetic friction only (as shown in figs. 4c) and d)), but also the size of each cluster is much larger. The common feature for all systems is a significant modification of the force networks with increasing ρ beyond jamming transition. To our knowledge this finding has not been yet reported in the literature.

Before discussing in some more detail the monodisperse system with kinetic friction, we comment on the connection between B0 and Z, which we briefly mentioned when considering polydisperse system, $r_p = 0.2$, with kinetic friction, see fig. 2c). To analyze this connection, we consider additional systems, with $r_p = 0.1, 0.3, 0.4$ and $\mu = 0.0, 0.1, 0.2, 0.4$ (static friction only). First, we identify the force threshold, $\bar{F}m(\rho)$, maximizing B0(ρ). Then we consider $\mathrm{B0}(\rho; \bar{F})_{\bar{F}=\bar{F}m(\rho)}$), and identify ρ_c as the ρ corresponding to the inflection point on this curve. By comparing with the curve $Z(\rho)$, we find that the inflection points of these two curves occur, within the accuracy of our data, at the same ρ_c's for all considered systems. Identifying now ρ_c as the jamming packing fraction, we conjecture that at jamming transition the force network evolves the fastest as the packing fraction changes. For the systems considered, we find that ρ_c is a monotonically decreasing function of r_p and μ, with $0.79 \lessapprox \rho_c \lessapprox 0.83$ as μ varies and $r_p = 0.2$, and $0.785 \lessapprox \rho_c \lessapprox 0.81$ as r_p varies and $\mu = 0.5$. To put these results in perspective, we note that the values for ρ_c are consistent with, although slightly smaller than the ones reported in recent experiments with compressed photoelastic particles [20].

Finally we discuss why monodisperse systems with kinetic friction only show such different behavior compared to the other three systems considered. Figures 6a) and b) as well as attached animations (`fig6a-animation.mov` and `fig6b-animation.mov`) provide a qualitative explanation: the comparison of normal force snapshots of the two monodisperse systems suggest a more uniform force network if only kinetic friction is present (panel b)), although it should be noted that this visual observation can be easily "clouded" by using a different color scheme, which would show that there is still an elaborate force network structure in the parts of domains which appear uniform in the present figure; this structure involves however smaller range of forces compared to the other systems considered. This increased uniformity suggests a smaller number of connected components, consistent with the B0's shown in fig. 4. Of course, B0's provide a much more precise measure of this uniformity. We have also computed

force-force correlation functions to check whether this measure would clearly suggest that the structure of the two systems is significantly different, but were not able to observe a clear signature of the difference. However, additional information can be found by considering the radial distribution function, $g(r)$, and the number of contacts, shown in fig. 6c) and d). Based on values of Z for large ρ, we see larger number of contacts for kinetic friction only, and based on $g(r)$ we see better defined correlations between the particle positions, suggesting partial crystallization for monodisperse system with kinetic friction. Consistent results regarding the influence of friction on structural ordering were reported previously [21–23]. Therefore, the results obtained based on B0's are found to be consistent with what may be concluded, based on more standard measures, and the comparison of B0's obtained for large ρ's between different systems can be used to detect order. However, the insight obtained by considering B0's is significantly more complete, since they provide information not only about particle positions and ordering, but also about the force networks' structure. For example, $g(r)$'s for polydisperse systems with static or kinetic friction are similar, but the average cluster size for large ρ are significantly different.

Conclusions. – In this letter, we have shown that the simplest of the topological measures, the Betti numbers, when used together with established techniques, provide significant new insight into the properties of force networks. In addition, measures such as B0 and B1 can be used to define the properties of force networks in a precise and objective manner. For brevity, here we have concentrated mostly on B0, and already this measure has allowed to make a significant progress. In particular, we find that in the systems with strong static friction (large Coulomb threshold), the influence of polydispersity on force network structure appears to be minor: polydispersity leads to an only slightly increased number of components/clusters for large packing fractions. In the systems described by a kinetic friction model, the influence of polydispersity is dramatically different: here monodisperse systems are characterized by significantly more uniform force networks for large packing fractions, compared to polydisperse systems. We have shown that this increased uniformity is related to partial crystallization. By following the evolution of the system as it is being compressed, we find that increased uniformity of the force network in the monodisperse system with kinetic friction emerges at the packing fractions which are larger than the one characterizing jamming transition. Therefore, friction has a dramatic effect on the structure of force networks (and on spatial ordering) for strongly compressed monodisperse systems. For polydisperse systems, we find that static friction leads to a larger number of smaller clusters compared to the systems modeled by kinetic friction with the same Coulomb threshold. These findings were made possible by utilizing precise and well-defined topological measures, which allow to clearly distinguish the properties of force networks in different systems. In the future works, these measures will be used to quantify the similarities and differences between results of different simulations, and more importantly, between simulations and experiments.

* * *

This work was partially supported by NSF DMS-0835611 and DTRA 1-10-1-0021 (LK, AG), and NSF-DMS-0915019, 0835621, 1125174, AFOSR and DARPA (KM, MK).

REFERENCES

[1] Liu A. J. and Nagel S. R., *Jamming and Rheology* (Taylor & Francis, London, New York) 2001.
[2] Majmudar T. S. and Behringer R. P., *Nature*, **435** (2005) 1079.
[3] Goldman D. I. and Umbanhowar P., *Phys. Rev. E*, **77** (2008) 021308.
[4] Radjai F., Jean M., Moreau J. J. and Roux S., *Phys. Rev. Lett.*, **77** (1996) 274.
[5] Silbert L. E., Grest G. S. and Landry J. W., *Phys. Rev. E*, **66** (2002) 061303.
[6] Peters J., Muthuswamy M., Wibowo J. and Tordesillas A., *Phys. Rev. E*, **72** (2005) 041307.
[7] Tordesillas A., Walker D. M. and Lin Q., *Phys. Rev. E*, **81** (2010) 011302.
[8] Ostojic S., Somfai E. and Nienhuis B., *Nature*, **439** (2006) 828.
[9] Staufer D. and Aharonov A., *Introduction to Percolation Theory* (Taylor & Francis, Philadelphia) 2003.
[10] Arévalo R., Zuriguel I. and Maza D., *Phys. Rev. E*, **81** (2010) 041302.
[11] Geng J., Behringer R. P., Reydellet G. and Clément E., *Physica D*, **182** (2003) 274.
[12] Kondic L., *Phys. Rev. E*, **60** (1999) 751.
[13] Cundall P. A. and Strack O. D. L., *Géotechnique*, **29** (1979) 47.
[14] Brendel L. and Dippel S., *Lasting contacts in molecular dynamics simulations*, in *Proceedings of Physics of Dry Granular Media*, edited by Herrmann H. J., Hovi J.-P. and Luding S. (Kluwer Academic Publishers, Dordrecht) 1998, p. 313.
[15] Luding S., *Granular Matter*, **10** (2008) 235.
[16] Goldenberg C. and Goldhirsch I., *Nature*, **435** (2005) 188.
[17] Kacynksi T. and Mischaikow K., *Computational Homology* (Springer, New York) 2004.
[18] Mischaikow K., Computational Homology Project, `http://chomp.rutgers.edu/`.
[19] Kondic L., Plots of B1 can be found here: `http://m.njit.edu/~kondic/kondic-etal-epl2012.pdf`.
[20] Majmudar T., Sperl M., Luding S. and Behringer R. P., *Phys. Rev. Lett.*, **98** (2007) 058001.
[21] Silbert L. E., Ertaz D., Grest G. S., Halsey T. C. and Levine D., *Phys. Rev. E*, **65** (2002) 031304.
[22] Donev A., Torquato S., Stillinger F. and Connelly R., *J. Appl. Phys.*, **95** (2004) 989.
[23] Xu N., Blawzdziewicz J. and O'Hern C. S., *Phys. Rev. E*, **71** (2005) 061306.